Kinetics of bidirectional H^+ and substrate transport by the proton-dependent amino acid symporter PAT1

Martin FOLTZ, Manuela MERTL, Veronika DIETZ, Michael BOLL, Gabor KOTTRA and Hannelore DANIEL[1]

Molecular Nutrition Unit, Institute of Nutritional Sciences, Center of Life and Food Sciences, Technical University of Munich, Hochfeldweg 2, D-85350 Freising-Weihenstephan, Federal Republic of Germany

PAT1 is a recently identified member of the PAT family of proton/amino acid co-transporters with predominant expression in the plasma membrane of enterocytes and in lysosomal membranes of neurons. Previous studies in *Xenopus* oocytes expressing PAT1 established proton/substrate co-transport associated with positive inward currents for a variety of small neutral amino acids. Here we provide a detailed analysis of the transport mode of the murine PAT1 in oocytes using the two-electrode voltage-clamp technique to measure steady-state and pre-steady-state currents. The GPC (giant patch clamp) technique and efflux studies were employed to characterize the reversed transport mode. Kinetic parameters [K_m (Michaelis constant) and I_{max} (maximum current)] for transport of various substrates revealed a dependence on membrane potential: hyperpolarization increases the substrate affinity and maximal transport velocity. Proton affinity for interaction with PAT1 is almost 100 nM, corresponding to a pH of 7.0 and is independent of substrate. Kinetic analysis revealed that binding of proton most likely occurs before substrate binding and that the proton and substrate are translocated in a simultaneous step. No evidence for a substrate-uncoupled proton shunt was observed. As shown by efflux studies and current measurements by the GPC technique, PAT1 allows bidirectional amino acid transport. Surprisingly, PAT1 exhibits no pre-steady-state currents in the absence of substrate, even at low temperatures, and therefore PAT1 takes an exceptional position among the ion-coupled co-transporters.

Key words: efflux characteristics, electrophysiology, giant patch clamp, pre-steady-state currents, proton/amino acid transporter, *Xenopus laevis* oocytes.

INTRODUCTION

Although some basic features of the mammalian proton-coupled amino-acid-transport protein PAT1 have been reported, a detailed analysis of the mode by which the protein couples transmembrane amino acid flux to movement of protons has not been performed.

Proton-coupled amino acid transport across biological membranes is a common phenomenon in prokaryotes and lower eukaryotes [1]. However, in mammalian species, such proton-coupled amino-acid-transporting systems are scarce. On the basis of work in isolated vesicles from brush-border membranes of kidney, the first evidence for the presence of proton-coupled transporters for small polar amino acids was obtained in the late 1980s and 1990s [2–4]. Similarly, in the human intestinal cell line Caco-2, the existence of a proton-coupled system capable of transporting glycine, alanine, β-alanine, proline and amino acid derivatives such as GABA (γ-aminobutyric acid), and D-cycloserine was demonstrated [5–9], and these systems have been termed 'PAT' (**p**roton-dependent **a**mino acid **t**ransporters).

The molecular entities of this transporter family have been identified and, in the recent years, four different transporter cDNAs (PAT1–PAT4) have been cloned [10]. All members represent proteins with 483–500 amino acid residues, with a predicted 11 transmembrane domains and a mean similarity of $> 65\,\%$ to each other. Whereas two of the proteins still are orphan transporters, PAT1 and PAT2 proteins have been functionally characterized as proton-coupled symporters. PAT1, cloned so far from rat, mouse and human [10–13], appear to represent the functionally identified PAT systems from the apical membranes of the enterocytes and renal proximal-tubular epithelial cells. In fact, the human PAT1 cDNA has been cloned from the human intestinal cell line Caco-2, and the PAT1 protein could be localized in the apical membrane of Caco-2 cells [12]. The cDNA of PAT1 was initially cloned from rat brain, and the protein was found in lysosomal membranes of neuronal cells by immunohistochemistry [13]. Here the transporter is proposed to mediate lysosomal export of small amino acids from intralysosomal protein breakdown. In primary neuronal cells prepared from rat hippocampus the transporter localizes to specific plasma-membrane domains called the 'exocyst complex' [14]. Whether this finding is of significance *in vivo* in the developing or mature brain in the neuronal uptake or release of neurotransmitters such as glycine and GABA – both PAT1 substrates – is so far not known.

The basic functional properties of PAT1 when heterologously expressed have been elucidated in COS-7 and HeLa cells and in *Xenopus laevis* oocytes. The substrate specificity is well described and, besides small L-α-amino acids (glycine, alanine and proline), certain β- and γ-amino acids (e.g. β-alanine and GABA), D-amino acids (e.g. D-serine and D-alanine) and osmolytes such as sarcosine (*N*-methylglycine) and betaine (*N*-trimethylglycine), were also shown to be transported. Critical structural features of substrates that show electrogenic transport by PAT1 are a short length of the amino acid side chain, a free negatively charged (carboxy) group and a short spacing between the amino and carboxy group, whereas a free amino group is not essential for PAT1 interaction [15].

PAT1-mediated transport is highly dependent on the extracellular pH and on membrane potential. The transport of protons

Abbreviations used: GABA, γ-aminobutyric acid; GPC, giant patch clamp; NHE3, Na^+/H^+ exchanger isoform 3; PAT, proton/amino acid transporter; PEPT1, peptide transporter 1; TEVC, two-electrode voltage clamp; V_m, membrane potential.

[1] To whom correspondence should be addressed (email daniel@wzw.tum.de).

and the zwitterionic form of amino acid substrates is electrogenic, with a stoichiometry of 1:1, the latter being shown for the model substrate L-proline. Substrate-dependent proton translocation by PAT1 has been directly shown by recording intracellular acidification in oocytes expressing PAT1 [11].

Here we present a more detailed analysis of the transport mode of the murine PAT1 protein expressed in *X. laevis* oocytes. By recording steady-state currents, the transport characteristics of different substrates have been analysed with respect to substrate- and proton-binding affinities and their dependence on membrane potential. Moreover, the ability of PAT1 for bidirectional transport and the asymmetry of the binding site in the inward- and outward-facing direction is demonstrated for the first time, and an analysis of pre-steady-state currents is provided. The results help us to understand amino acid transport by PAT1 in its different locations, such as lysosomal membranes or the brush border of epithelial cells.

MATERIALS AND METHODS

Materials

South African clawed frogs (*Xenopus laevis*) were purchased from Nasco (Fort Atkinson, WI, U.S.A.). All experiments with *X. laevis* were approved by the Bavarian state ethics committee and followed the German guidelines for care and handling of laboratory animals. Amino acids and related compounds were obtained from Sigma Chemie (Deisenhofen, Germany) or Merck (Darmstadt, Germany) in *pro analysi* quality. L-[3,4-^{3}H]Proline (60 Ci/mmol) was purchased from Amersham Biosciences (Freiburg, Germany). Collagenase A was obtained from Roche Molecular Biochemicals (Mannheim, Germany).

X. laevis oocyte handling and cRNA injection

Oocytes were treated with collagenase A (Roche Diagnostics) for 1.5–2 h at room temperature in Ca^{2+}-free ORII solution (82.5 mM NaCl/2 mM KCl/1 mM $MgCl_2$/10 mM Hepes, pH 7.5) to remove follicular cells. After sorting, healthy oocytes of stages V and VI were kept at 18 °C in modified Barth solution containing 88 mM NaCl, 1 mM KCl, 0.8 mM $MgSO_4$, 0.4 mM $CaCl_2$, 0.3 mM $Ca(NO_3)_2$, 2.4 mM $NaHCO_3$ and 10 mM Hepes, pH 7.5. The next day, oocytes were injected with 27 nl of sterile water (control), 27 nl of murine PAT1 cRNA or 13 nl of rabbit PEPT1 (peptide transporter 1) cRNA (10 ng of cRNA/oocyte respectively) and were kept in modified Barth solution at 18 °C until further use (3–5 days after injection).

TEVC (two-electrode voltage clamp)

TEVC experiments were performed as described previously [11]. Briefly, the oocyte was placed in an open chamber and continuously superfused with incubation buffer (100 mM choline chloride/2 mM KCl/1 mM $MgCl_2$/1 mM $CaCl_2$/10 mM Mes or Hepes, pH 5.5–8.5) in the absence or presence of the substances studied. Oocytes were voltage-clamped at -60 mV using a TEC-05 amplifier (NPI Electronic, Tamm, Germany) and current–voltage (I–V) relationships were measured using short (100 ms) pulses separated by 200 ms pauses in the potential range -160 to $+80$ mV. I–V measurements were made immediately before, and 20–30 s after, substrate application, when current flow reached steady state. The current evoked by PAT1 at a given membrane potential was calculated as the difference between the currents measured in the presence and the absence of substrate. Positive currents denote positive charges flowing out of the oocyte (see Figures 6 and 8 below).

The kinetics of substrate-dependent currents were constructed from experiments employing five different amino acid concentrations in Na^+-free buffer at pH 6.5, with at least eight individual oocytes expressing PAT1 from at least two different oocyte batches for each substrate. Substrate-evoked currents of a single experiment were transformed by the Eadie–Hofstee method and, after linear regression analysis, the substrate concentration that cause half-maximal transport activity were derived. Transport parameters, defined by apparent K_m (Michaelis constant in mM) and I_{max} (maximum current in nA), are shown as means $\pm$ S.E.M. for eight oocytes.

The kinetics for proton interaction with PAT1 were obtained under conditions of substrate saturation (50 mM). Such high concentrations were chosen to exclude pH effects on the titration of the substrate over the pH range used and to allow, even at the lowest pH (5.5), substrate saturation for the zwitterionic species. Substrate-free buffer was, for comparison, osmotically adjusted with 50 mM mannitol. The standard incubation medium was buffered with 10 mM Hepes (> pH 6.0) or Mes (pH < 6.0) and adjusted in the presence of substrate to the respective pH values. Apparent K_m values were derived from individual experiments by linear regression analysis from Eadie–Hofstee transformations of inward currents determined as a function of six different apparent proton concentrations. Values provided in the text, Tables or Figures represent the means $\pm$ S.E.M for 11 different determinations. It is noteworthy that the data points could always be fitted best to single-step kinetics, with no indication for unspecific proton binding effects or an allosteric proton-binding mechanism.

GPC (giant patch clamp) experiments

GPC experiments were performed as described previously [16]. Patch pipettes of 20–30 μm diameter were prepared from thin-walled borosilicate glass capillaries [MTW-150; World Precision Instruments (WPI), Berlin, Germany] and were filled with a solution containing (in mM) NaCl (10), sodium isethionate (80), $MgSO_4$ (1), $Ca(NO_3)_2$ (1) and Hepes (10) titrated to pH 7.5 and connected to an EPC-9 amplifier (HEKA, Lambrecht, Germany). After removal of the vitelline layer and gigaseal (1–10 gΩ) formation, pipettes were moved to a perfusion chamber and continuously superfused with the control bath solution composed of (in mM) potassium aspartate (100), KCl (20), $MgCl_2$ (4), EGTA (2) and Hepes (10), pH 7.5. During experiments, the membrane potential was clamped to 30 mV, and I–V relationships in the potential range of -80 to $+60$ mV were measured in the same way as described for TEVC experiments. The data were recorded with PULSE software (HEKA) and evaluated with the PATCH software program (courtesy of Dr Bernd Letz, HEKA).

The transport parameters K_m (mM) and I_{max} (pA) were obtained from least-square fits to the Michaelis–Menten equation. Since I_{max} values depend on the expression level of the transporter, all parameters (altered substrate concentrations and pH) were always analysed in the same oocyte. This required a decrease in the number of data points for analysis to five in these experiments with concentrations of 1, 2.5, 5, 10 and 20 mM for all substrates at pH 7.5.

Pre-steady-state measurements

Pre-steady-state currents were measured with the same equipment and similarly to the recordings of the I–V relations. The membrane potential was stepped from the holding potential of -60 mV to -160 to $+80$ mV in 40 mV steps; however, the pulse length was only 40 ms, and the recorded signals were low-pass-filtered at

1 kHz. To obtain a good resolution of both the high-amplitude current peak, loading the membrane capacitance, and the low-amplitude pre-steady-state component, the current was recorded first with low amplification (0.2 V/μA) and then with high amplification (1 V/μA). The time resolution was, for both runs, 0.16 ms. In the high-amplification mode the peaks of the capacitive currents were cut off by the analogue-to-digital conversion. To decrease measurement noise, five runs with each setting were recorded, stored and averaged. The data were evaluated offline by using self-written programs in VBA for Excel and using the Solver routine for least-square fitting. After averaging the data the following function containing two exponential relaxations was fitted to the data points recorded with the low amplification:

$$I_{v,t} = I_{\mathrm{cap},v} \cdot \exp(-t/\tau_{\mathrm{cap},v}) + I_{\mathrm{pre},v} \cdot \exp(-t/\tau_{\mathrm{pre},v}) + I_{\mathrm{s},v}$$

where $I_{v,t}$ is current at the membrane potential v and at time t, $I_{\mathrm{cap},v}$ is the peak capacitive current at v, $\tau_{\mathrm{cap},v}$ is the time constant of the capacitive current component at v, $I_{\mathrm{pre},v}$ is the peak pre-steady-state current at v, $\tau_{\mathrm{pre},v}$ is the time constant of the pre-steady-state current component at v, and $I_{\mathrm{s},v}$ is the steady (direct current) component of the current at v.

Owing to the limited speed of the voltage clamp, the first 1.12 ms of the current records (i.e. the first seven data points) were omitted from the fit procedure. When the best fit with the low amplification data was reached, the parameters $I_{\mathrm{pre},v}$, $\tau_{\mathrm{pre},v}$ and $I_{\mathrm{s},v}$ were then refitted using the data points recorded with the high amplification, whereas the parameters $I_{\mathrm{cap},v}$ and $\tau_{\mathrm{cap},v}$ were fixed at the values obtained in the previous fit. The charge movement due to pre-steady-state currents at v was calculated as the time integral of the relaxation function.

For analysis at low temperatures, the measuring chamber was perfused with solutions cooled down from the room temperature (22 °C) to about 10 °C. This was achieved by filling cooled solutions into thermically isolated reservoirs and by further cooling the perfusate with a Peltier element (heat pump) in the very neighbourhood of the chamber. In a part of the experiments the temperature was measured at the chamber outflow, and a solution temperature of about 10 °C or lower was verified.

Efflux measurements

Eight oocytes (injected with water or cRNA) per experiment were injected with 100 μM L-[3,4-^{3}H]proline (2.5 nCi/oocyte) in efflux buffer (100 mM choline chloride/2 mM KCl/1 mM $MgCl_2$/1 mM $CaCl_2$/10 mM Hepes, pH 7.5). After 1 min of regeneration at room temperature in efflux buffer, oocytes were briefly washed and immediately transferred to individual wells of a 96-well plate (0.5 ml volume/well). A 200 μl volume of standard incubation buffer was added with a multichannel pipette. After the indicated time intervals, 100 μl of medium was withdrawn for the determination of radioactivity and replaced by new buffer. At the end of the experiment, oocytes were solubilized by adding 100 μl of 10 % (w/v) SDS. Radioactivity of the efflux buffer at the different time points, and in the oocyte, was counted by liquid scintillation.

Statistics

All calculations (linear as well as non-linear regression analyses) were performed using Prism software (GraphPad, San Diego, CA, U.S.A.). Transport measurements in *Xenopus* oocytes were performed with at least eight oocytes from two different oocyte batches. Data are presented as means ± S.E.M. Statistically significant differences were determined using ANOVA, followed by Newman–Keuls multiple comparison test.

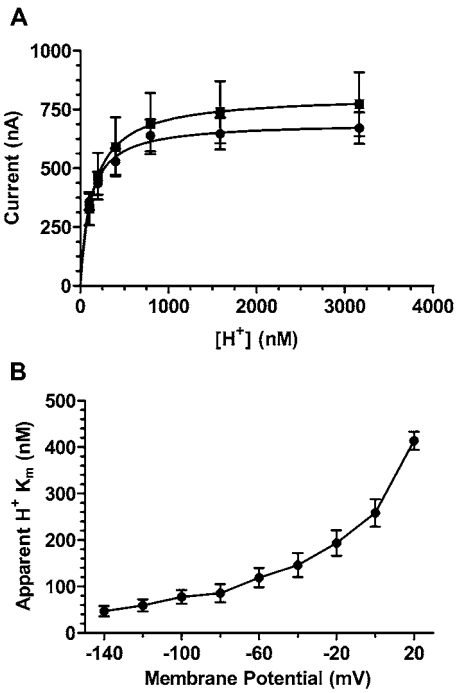

Figure 1 Kinetics of proton-dependent activation of amino acid induced steady-state currents in *X. laevis* oocytes expressing PAT1

(**A**) Currents induced by 50 mM glycine (■) and 50 mM GABA (●) were determined as a function of the extracellular H^+ concentration in the concentration range of 100 nM (pH 7.0)–3.1 μM (pH 5.5). Data are presented as means ± S.E.M. ($n = 11$). (**B**) Apparent $K_m^{H^+}$ value as a function of membrane potential determined in the presence of 50 mM glycine. K_m values are shown as means ± S.E.M. of 11 independent determinations.

RESULTS

H^+/amino acid steady-state kinetics

Proton activation constants

We first determined the affinity for proton interaction ($K_m^{H^+}$) with PAT1 under saturating substrate concentrations (50 mM) by varying the extracellular pH from pH 7.0 to 5.5. As shown in Figure 1(A), proton-dependent inward currents followed typical Michaelis–Menten kinetics, with apparent $K_m^{H^+}$ values of 133 ± 4.3 nM in the case of glycine and 111 ± 6.8 nM in the presence of GABA. The determined $K_m^{H^+}$ values were independent of the amino acid substrate, as they did not significantly differ from each other ($P > 0.05$). When currents were recorded at different membrane voltages, the apparent proton affinity with glycine as substrate decreased nearly 9-fold by depolarizing the membrane from −140 mV to +20 mV (Figure 1B). Interestingly, the $I_m^{H^+}$ values for proton-dependent glycine transport at saturating substrate concentrations decreased only 2.4-fold by depolarization from −140 mV to +20 mV (results not shown).

Voltage-dependence

To determine the effect of membrane voltage on the kinetic parameters K_m and I_{max} of PAT1 substrates, inward currents were recorded as a function of increasing L-alanine concentrations (0.2–20 mM). Figure 2(A) demonstrates that, under non-saturating substrate concentrations, inward currents almost linearly depend on membrane potential and only at 20 mM L-alanine do currents show a tendency towards saturation at negative membrane potentials. A comparative analysis of membrane voltage effects on the K_m

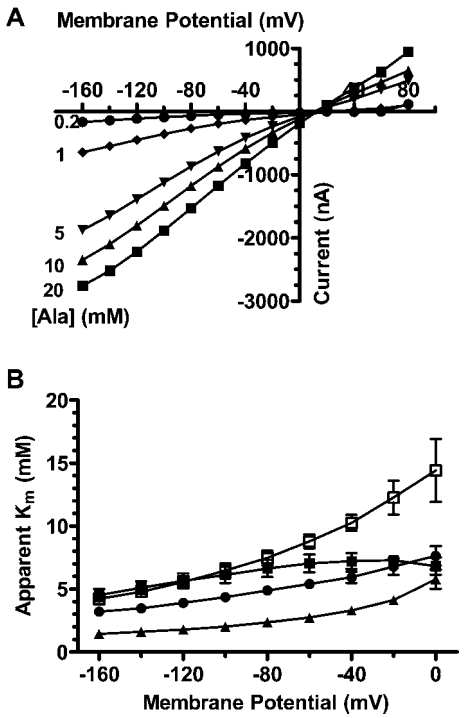

Figure 2 Apparent substrate affinities of PAT1-mediated transport currents as a function of membrane potential

(**A**) Representative PAT1-mediated inward currents induced by different L-alanine concentrations (0.2 mM–20 mM) at pH_{out} 6.5 as a function of membrane potential. (**B**) Apparent substrate affinity constants of glycine (■), proline (▲), taurine (□) and betaine (●) as a function of membrane potential in oocytes expressing PAT1, determined by TEVC in Na^+-free perfusion solutions at pH 6.5. Data represent the K_m values derived from Eadie–Hofstee transformations of inward currents as a function of substrate concentration and are represented as means ± S.E.M. for eight oocytes. Where error bars are not visible, the S.E.M. values are smaller than symbols.

values for glycine, L-proline, betaine and taurine is provided in Figure 2(B). Membrane depolarization had only a minor effect on the affinity of glycine, with a decline in the K_m value of about 1.5-fold and, similarly, L-alanine and β-alanine affinities only modestly changed (results not shown). Affinities of L-proline, betaine and taurine decreased between 2.1- and 4.1-fold by shifting the membrane potential from − 160 mV to 0 mV (Figure 2B), and similar changes in apparent K_m were obtained for D-proline, D-alanine, sarcosine and GABA (results not shown). All I_{max} values for the different substrates decreased by 70–80 % when the membrane voltage was changed from − 160 mV to 0 mV (results not shown).

Order of binding

For assessing whether binding of protons and amino acids to PAT1 follows an ordered or random mechanism, we determined apparent K_m^{Gly} and I_m^{Gly} at two different pH values (pH 6.5 = 0.316 μM H^+ and pH 5.0 = 10 μM H^+). At both pH values substrate-dependent inward currents showed simple Michaelis–Menten kinetics, and decreasing the external pH from pH 6.5 to 5.0 did not significantly change I_{max} but decreased K_m^{Gly} significantly ($P < 0.001$) (Figures 3A and 3B, and Table 1). When currents were determined at two different glycine concentrations in dependence of the external H^+ concentration (pH 7.0 to 5.5), the apparent $K_m^{H^+}$ for proton binding increased more than 4.4-fold and the proton-dependent $I_m^{H^+}$ increased 2.3-fold when the glycine concentration was increased from 2 to 20 mM (Figures 3C and 3D, and Table 1). These data strongly suggest that there is an ordered

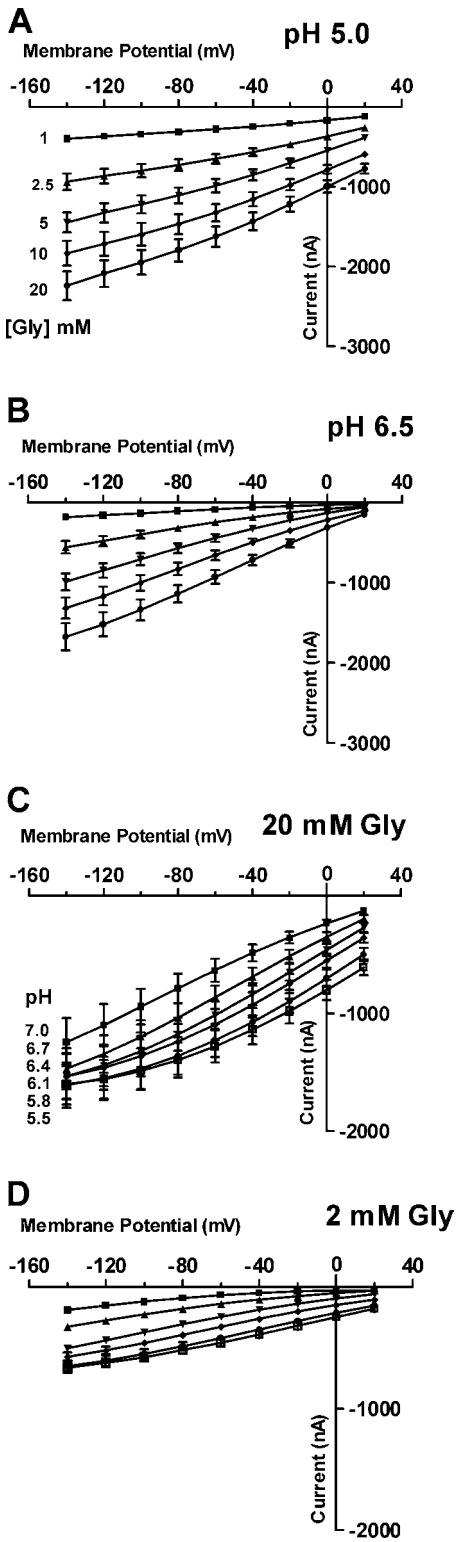

Figure 3 PAT1-mediated inward currents induced by different substrate concentrations and varying pH_{out} as a function of membrane potential

(**A** and **B**) Currents recorded at six different concentrations of glycine (1–20 mM) at extracellular pH 5.0 (**A**), or pH 6.5 (**B**) as a function of membrane potential. (**C** and **D**) Proton-dependent kinetics of glycine-induced currents determined at six different pH values ranging from pH 7.0 to pH 5.5 in the presence of either 20 mM glycine (**C**) or 2 mM glycine (**D**) as a function of membrane potential. Data are the means ± S.E.M. of average currents determined in six individual oocytes. The apparent K_m and I_{max} values derived from these experiments are compiled in Table 1.

Table 1 Kinetic constants for H^+-dependent and glycine-dependent transport currents as a function of membrane potential

The apparent K_m values for glycine were determined in TEVC studies in individual oocytes at two different pH_{out} values (6.5 and 5.0) using five different glycine concentrations (1–20 mM). Additionally, apparent proton affinity constants (K_m^{H+}) were determined in individual oocytes at two different glycine concentrations (2 and 20 mM) and at pH values varying between 7.0 and 5.0. Substrate-induced currents were transformed by the Eadie–Hofstee method, and K_m and I_{max} values were calculated by linear regression analysis. Maximum currents are normalized to the maximum current observed in an individual oocyte at pH_{out} 6.5 ($I_{max}/I_{max,pH6.5}$) (a) or at 2 mM glycine ($I_{max}/I_{max,[Gly]2mM}$) (b). K_m and I_{max} values are presented as the means ± S.E.M. for at least six independent experiments.

(a)

Condition	V_m (mV)	K_m^{Gly} (mM)	$I_{max}/I_{max,pH\ 6.5}$
pH 6.5	−100	9.6 ± 0.5	1
	−60	13.1 ± 1.0	1
	−20	13.5 ± 1.4	1
pH 5.0	−100	5.5 ± 0.6	1.26 ± 0.10
	−60	6.0 ± 0.6	1.40 ± 0.12
	−20	6.4 ± 0.5	1.55 ± 0.09

(b)

Condition	V_m (mV)	K_m^{H+} (nM)	$I_{max}/I_{max,[Gly]2mM}$
2 mM glycine	−100	361 ± 38	1
	−60	554 ± 61	1
	−20	861 ± 80	1
20 mM glycine	−100	77 ± 15	2.37 ± 0.28
	−60	130 ± 18	2.45 ± 0.29
	−20	194 ± 27	2.37 ± 0.25

binding mechanism, with the protons binding first, followed by substrate, as addressed specifically in the Discussion.

No-substrate uncoupled proton conductance

We also addressed the question of whether PAT1 exhibits a proton conductance in the absence of amino acid substrates. For this, *I–V* relationships were recorded in oocytes expressing PAT1 and in water-injected controls. Oocytes were perfused with buffer solutions at various H^+ concentrations (pH 7.0–5.5) in the absence of amino acids. Figures 4(A) and 4(B) demonstrate, on the basis of *I–V* relationships, and Figure 4(C), by intracellular pH recordings, that alterations in extracellular pH over a large range does not cause a proton or charge influx different from the changes observed in water-injected control oocytes. We also calculated by linear regression analysis the reversal potential at each pH value tested. Only a slight conversion into less negative potentials, from −31 ± 2.5 mV (pH 7.5) to −27 ± 1.5 mV (pH 5.0), was observed in oocytes expressing PAT1 (Figure 4A). However, this shift was not significantly different ($P > 0.05$) from that obtained in control oocytes (−23 ± 1.6 mV to −20 ± 1.2 mV) (Figure 4B). These observations argue against the ability of PAT1 to translocate protons in the absence of amino acids.

Pre-steady-state kinetics

Analysis of pre-steady-state currents of other electrogenic ion-coupled solute transporters has been very helpful in defining their transport mode. We have determined for the first time the pre-steady-state currents of PAT1 in direct comparison with PEPT1 as another proton-dependent electrogenic symporter. Figure 5 shows typical current records in response to potential steps for

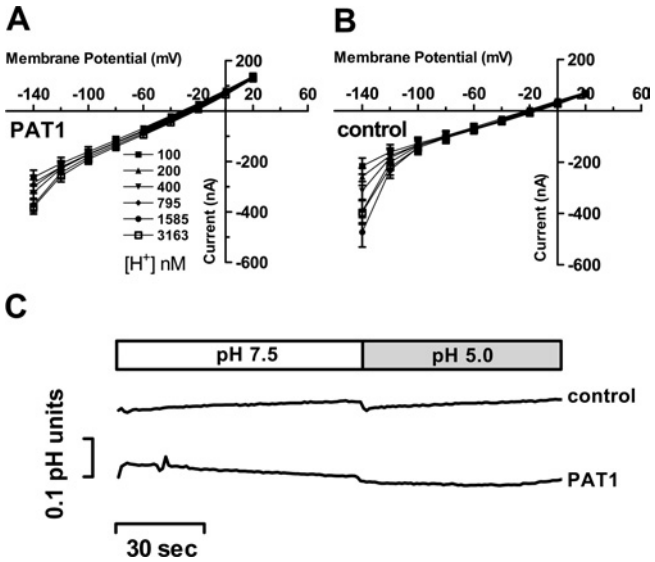

Figure 4 Recordings of *I–V* relationships and intracellular pH changes in oocytes expressing PAT1 in the absence of amino acid substrates

(**A** and **B**) Inward currents recorded in oocytes expressing PAT1 (**A**) or water (**B**) injected controls were perfused with Na^+-free buffer solutions of six different pH values (pH 7.0–5.5). Oocytes were clamped to −40 mV, and *I–V* relationships were recorded in the potential range between +20 mV and −140 mV. At the end of the experiment, oocytes expressing PAT1 were perfused with 20 mM GABA at pH 5.5 and inward currents of 900 ± 89 nA were obtained, demonstrating the functional PAT1 expression level. No significant changes in the reversal potential could be determined between water-injected and PAT-expressing oocytes upon alterations in pH_{out} and membrane voltage. Data represent the means ± S.E.M. for at least eight oocytes in each experiment. (**C**) Representative intracellular pH changes (ΔpH) in oocytes injected with water or PAT1 cRNA and perfused with buffer pH 7.5 or pH 5.0 in the absence of substrate. Oocytes were clamped to −40 mV and intracellular pH, as well as holding currents, were recorded (holding currents are not shown). As a control, at the end of the experiment, the functional PAT1 expression level was determined by measuring the current and ΔpH induced by 20 mM glycine at pH 5.0 (current 1704 ± 169 nA; ΔpH 0.57 ± 0.15; $n = 3$).

PEPT1 and PAT1. In both cases, Figures 5(A) and 5(B) show the currents in the absence, and Figures 5(C) and 5(D) in the presence, of substrate. It becomes obvious that PEPT1-mediated currents show, in addition to the fast capacitive component, an additional potential-dependent slow component which disappears in the presence of substrate. No such slow component could be detected in case of PAT1, although the substrate-dependent steady-state current was even higher than that of PEPT1 (1206 as against 730 nA at −60 mV). These results were consistently found in at least seven oocytes from two donor animals in the same oocyte batch. The mean transport current observed in PAT1 cRNA-injected oocytes was 600 ± 83 nA (at −60 mV). The calculated pre-steady-state charge movement was, however, very small (0.74 ± 0.22 nC, $n = 7$ at −160 mV and pH 7.5), became still lower at pH 6.5 (0.55 ± 0.18 nC) and was not significantly different from zero at pH 5.5 (0.45 ± 0.21 nC). For comparison, the pre-steady-state charge transfer in oocytes expressing PEPT1 with a mean transport current of 450 ± 30 nA (at −60 mV) amounted to 16.6 ± 1.9 nC ($n = 16$) at −160 mV and pH 7.5.

In addition to the differences in the pre-steady-state charge movements, the time constants for the capacitive component were also different between PAT1 and PEPT1. For both transporters they were, as expected, independent of membrane potential, and averaged 0.393 ± 0.036 ms ($n = 7$) for PAT1 and 0.715 ± 0.059 ms for PEPT1.

One possible reason for the lack of significant pre-steady-state currents in PAT1 could be a very short time constant for the reorientation of the unloaded protein in the membrane in response

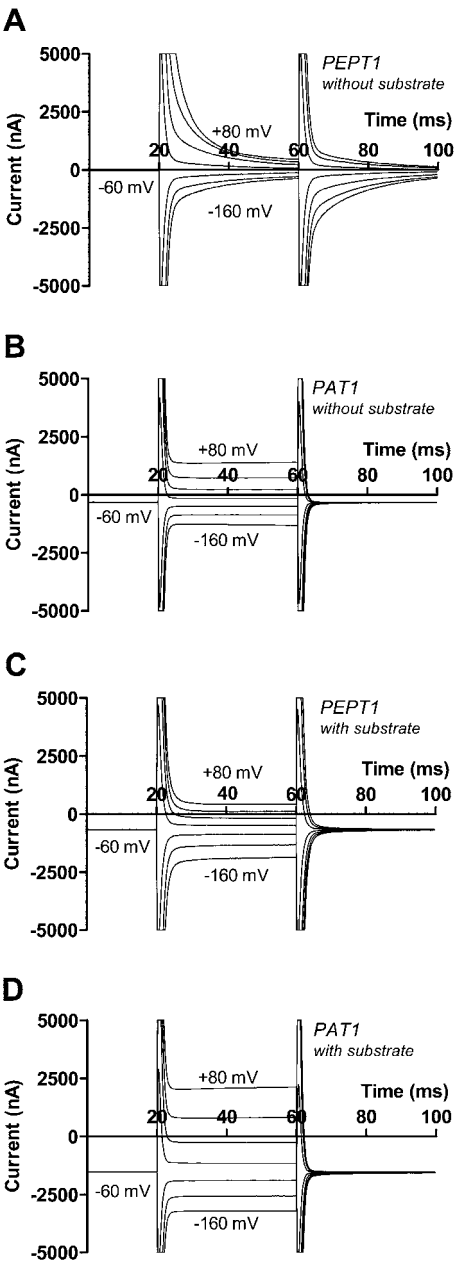

Figure 5 Comparative analysis of pre-steady state and steady state currents in oocytes expressing either PEPT1 and PAT1

(**A** and **B**) Current recordings in the absence of substrates for PEPT1 (**A**) and PAT1 (**B**) with fast capacitive current components obtained for both transporters, but a slow pre-steady-state current component present only in PEPT1. (**C** and **D**) Current recordings obtained in the presence of either 20 mM glycine-glutamine in case of PEPT1 (**C**) or 20 mM glycine in case of PAT1 (**D**) with increased steady-state currents observed for both transporters but the pre-steady-state component virtually completely suppressed only in the case of PEPT1. For further details, see the text.

to potential steps that than would be indistinguishable from the time constant of the capacitive currents. To better discriminate these two parameters, we performed the same experiments at low temperature. The results of seven identical experiments at low temperature revealed a decrease of transport currents from 594 ± 145 nA at room temperature to 165 ± 60 nA in the cooled state, thus reducing the turnover rate of the transporter by 77 ± 5 %. However, we did not observe any significant increase of a

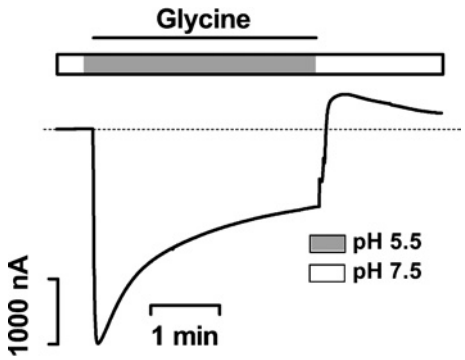

Figure 6 PAT1-mediated amino acid-induced outward transport currents measured in TEVC experiments

A representative current trace as obtained in an oocyte expressing PAT1 and clamped at -40 mV while it was continuously superfused for 4 min with 20 mM glycine at pH_{out} 5.5, followed by a fast wash-out with substrate-free buffer, pH 7.5.

current component with slow time constant (0.71 ± 0.34 nC at room temperature, 0.31 ± 0.17 nC at low temperature), demonstrating the lack of any detectable pre-steady-state currents in PAT1.

Bidirectional transport: PAT1-mediated amino acid efflux

For assessing whether PAT1 is also able to transport amino acids in the outward direction, we loaded oocytes expressing PAT1 with glycine and determined outwardly directed transport currents. As shown in Figure 6, PAT1-expressing oocytes were perfused at -40 mV with 20 mM glycine at pH 5.5 for 5 min while the inwardly directed current was recorded. A fast wash-out of substrate and a shift of external pH to 7.5 led to significant outward currents of up to 520 nA at a V_m (membrane potential) of -40 mV. These outward currents in the wash-out period were dependent on the PAT1 expression level and the length of substrate application period (results not shown). To confirm transport in the outward direction, efflux studies using radiolabelled proline were performed. After injection of oocytes with radiolabelled proline (5 nmol/oocyte), efflux of the tracer from oocytes expressing PAT1 was significantly higher that from control oocytes (Figure 7A). The presence of the extracellular substrates such as glycine or alanine increased efflux via PAT1 further by 1.9-fold (glycine) and 1.5-fold (alanine) as compared with the efflux in the absence of amino acids (Figure 7A). Proline efflux from preloaded oocytes followed Michaelis–Menten kinetics when determined as a function of extracellular glycine concentrations, with an apparent affinity constant for glycine of 1.6 ± 0.2 mM (Figure 7B).

To characterize in more detail the reversed transport mode of PAT1, we employed the GPC technique with membrane patches obtained from oocytes expressing PAT1. With increasing concentrations of D-alanine provided on the internal membrane side, outwardly directed currents were recorded, even at negative membrane potentials of -80 mV (Figure 8A). Like inward transport, outward transport currents were strongly dependent on membrane potential and increased from 1.1 ± 0.8 pA at -80 mV to 12.1 ± 2.8 pA at $+60$ mV in the presence of 50 mM D-alanine. No substrate-induced currents were observed in membrane patches obtained from control oocytes (results not shown). The amino-acid-induced outward currents followed typical Michaelis–Menten kinetics as a function of increasing concentrations of D-alanine (Figure 8B). We next determined apparent K_m values for different substrates from Michaelis–Menten kinetics of outward transport recorded at a membrane

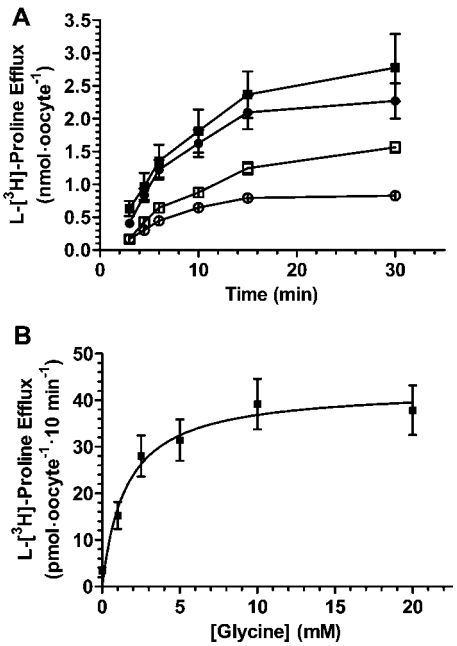

Figure 7 Demonstration of PAT1-mediated amino acid efflux

(**A**) Individual oocytes were injected with 5 nmol of L-proline (including 1pmol of L-[^{3}H]proline as a tracer) and efflux was measured in the absence (□) or the presence of 20 mM glycine (■) or alanine (●) in the incubation medium. Efflux of L-[^{3}H]proline from water-injected control oocytes is also shown (○). (**B**) PAT1-mediated efflux of proline from preloaded oocytes (injection of 5 nmol of L-proline, including 1 pmol of L-[^{3}H]proline per oocyte) as a function of increasing concentrations of glycine (1–20 mM) in the incubation buffer. Efflux rates of labelled L-proline were determined after 10 min of incubation under the various conditions and represent the means ± S.E.M. for at least eight oocytes per variable.

voltage of +60 mV. Affinities ranged from around 10 mM (L-proline and D-proline) to 45 mM (L-alanine) and were therefore almost 7-fold lower than the apparent K_m values for the same substrates as determined for the inward direction under the same conditions and at a membrane voltage of −60 mV (Figure 8C). As the most interesting observation, a significant linear relationship in affinities for substrate binding to PAT1 in its outward facing or its inward facing direction was observed. Affinities of substrates, such as proline or glycine, showed a dependence on membrane potential, with a decline at more negative voltages (Figure 8D). Additionally, maximal transport velocity determined for the outward direction exhibited a similar dependency on membrane potential as described for the inward direction. Alteration of membrane potential by 80 mV decreased the I_{max} values of all substrates tested between 40 and 60 % (results not shown).

DISCUSSION

Proton-dependent amino acid transport systems with selectivity for small neutral amino acids and their derivatives have been demonstrated in intestinal and renal epithelial cells [2–8], and it is now accepted that the PAT1 gene encodes the PAT activity in these epithelia [12]. We here provide an extended analysis of the functional characteristics of the PAT1 protein by electrophysiological measurements and by flux studies that do provide new and unexpected findings.

Proton and substrate affinity determinants of PAT1

The observed apparent proton affinity of about 100 nM corresponds to a pH of 7.0 and is almost 50-fold lower than proton affinity reported for the orthologue PAT2 [17]. Since the pH in the vicinity of the cell membrane is slightly acidic (pH 6.1–6.8) due to surface microclimate [18], PAT1 operates in intestinal epithelia most likely under proton saturation. On the basis of the functional coupling of proton recycling via NHE3 (Na^+/H^+ exchanger isoform 3) from the cytosol to the apical membranes, alterations in NHE3 activity can secondarily affect PAT transport activity, as shown in the Caco2-cell system [19]. In lysosomes of neurons, where PAT1 is also found, pH values of ⩽ pH 5.5 also would provide conditions allowing maximal rates for amino acid export [20]. We observed a strong voltage dependence of proton binding with the highest proton binding affinity at hyperpolarized voltages. Apparent affinities of amino acid substrates were also dependent on membrane potential, but with pronounced effects only at subsaturating proton concentrations (i.e. pH 6.5). The decrease in amino acid binding affinity at less negative potentials therefore reflects primarily the loss of the proton binding affinity.

PAT1 possesses an ordered-binding, simultaneous-transport, mode

The distinction of whether a symporter such as PAT1 possesses a random or ordered binding process is mainly based on competition between substrate and co-substrate and by assuming that the translocation of the protein across the cell membrane is the rate-limiting step in the transport cycle and not the binding of substrate and co-substrate [21,24]. Our observation that the proton affinity constants are essentially independent of the amino acid substrate (even though the amino acid K_m values are substantially different) suggests that PAT1 possesses an ordered binding mechanism, with protons binding first, followed by the amino acid. Under conditions of a rapid interfacial equilibrium, an ordered binding with the proton preceding the amino acid would mean that a state in which only the amino acid is bound to the transporter does not exist. Consequently the maximal transport currents at high glycine concentrations (I_{max}^{Gly}) should become independent of the proton concentration. Saturating glycine currents only barely responded to a 30-fold increase in H^+ concentration at low negative membrane potentials and became essentially independent of pH at hyperpolarized potentials. In contrast, the glycine concentration drastically affected both $I_{max}^{H^+}$ and $K_m^{H^+}$, consistent with amino acid binding following proton binding, as is also observed for other transporters [21–24], supporting an ordered binding mechanism.

Binding of proton and substrate is followed by a translocation step in which, most likely, H^+ and amino acid are simultaneously transported across the membrane. This is supported by the observation that, at least at potentials more positive than −100 mV, K_m^{Gly} increases at diminishing H^+ concentrations (e.g., at −60 mV, K_m^{Gly} increases strongly with increasing external pH; Table 1). In addition, the ratio I_{max}^{Gly}/K_m^{Gly} was strongly dependent on the external H^+ concentration, and this can be taken as additional evidence for an ordered-binding, simultaneous-transport model [21,25].

In this transport model of PAT1, an uncoupled H^+ influx can essentially be excluded on the basis of only minimal shifts in reversal potential in response to pH jumps and the lack of intracellular pH changes in the absence of substrates. The strong potential-dependence of apparent proton binding affinity may be explained by the 'ion-well' effect, i.e. that H^+ has to traverse a part of the transmembrane voltage in order to enter the proton-binding site [21]. In this respect PAT1 shares general features – such as the voltage-dependence of affinities, the ordered binding mechanism and the 'in-well' effect – with other symporters such as proton-coupled PEPT1, the Na^+-coupled hexose transporter SGLT1 (**s**odium-dependent **gl**ucose co-**t**ransporter 1) or the system A

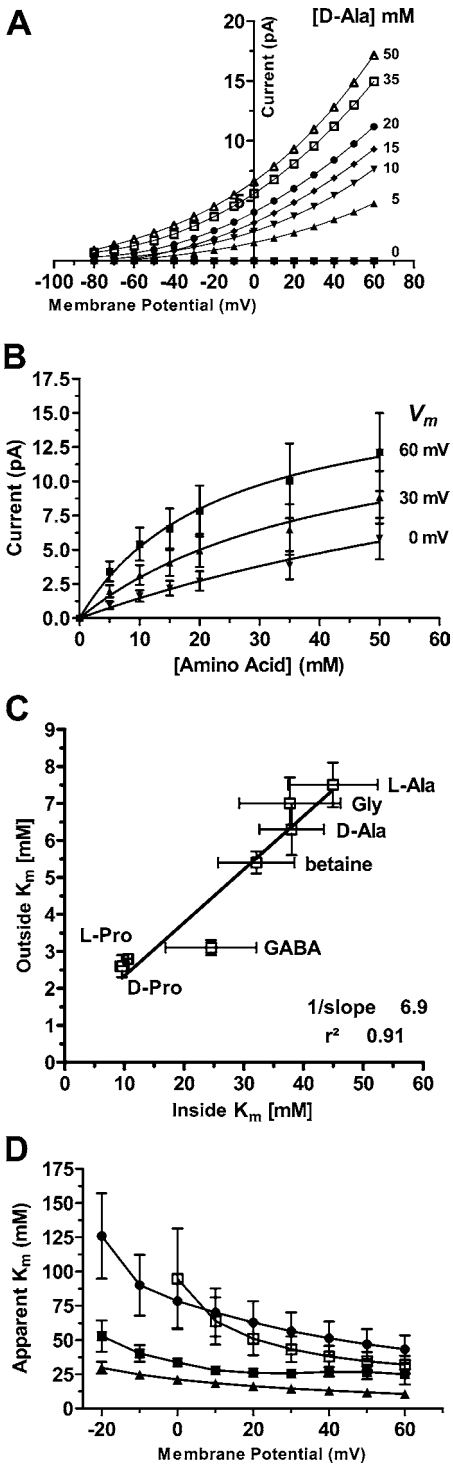

Figure 8 PAT1-mediated amino-acid-induced outward currents determined in GPC experiments

(**A**) Recording of an *I–V* relationship as difference curves in the presence and the absence of increasing concentrations of D-alanine (0–50 mM) at the cytosolic side in response to potential pulses between −80 and +60 mV. The pH of the buffer solutions was 7.5 on both sides of the membrane. (**B**) Kinetics of D-alanine-induced outward currents as a function of substrate concentration at pH 7.5 on both sides and holding potentials of +60 mV (■), +30 mV (▲) and 0 mV (▼). Means ± S.E.M. from six different oocytes are shown. Note that K_m values presented in the text and Tables are the means of constants as calculated from individual oocytes. (**C**) Apparent K_m values for a variety of substrates as derived from kinetic analysis of transport for the inward and outward directions. Transport currents for the outward direction were determined by the GPC technique in Na^+-free perfusion solutions containing the different substrates at a V_m of +60 mV (pH 7.5 at both sides). Transport currents for inward-directed transport were determined under the same experimental conditions in TEVC experiments in Na^+-free perfusion solutions containing the different substrates at a V_m of −60 mV (pH_{out} 7.5). On the basis of *I–V* relationships, K_m values were determined by fitting the data to the Michaelis–Menten equation. (**D**) Apparent K_m values for PAT1-mediated transport in the outward direction as a function of membrane potential. Results are means ± S.E.M. of at least six oocytes perfused with either glycine (■), proline (▲), betaine (□) or alanine (●). If error bars are not visible, the S.E.M. is smaller than symbol.

transporter SA2 [26–28], the latter belonging to the same superfamily as PAT1.

PAT1 lacks significant pre-steady-state currents

Analysis of pre-steady-state currents of PAT1 performed at room temperature and 10 °C yielded unexpected results. In contrast with most other ion-coupled transporter, and also in contrast with PEPT1, with significant potential- and pH-dependent pre-steady-state charge movements, in PAT1 these were virtually absent. There are two possible explanations for this lack of pre-steady-state charge movements. It could be that (a) PAT1 has an almost symmetric charge distribution within the protein that, in turn, would not produce a potential-dependent reorientation within the membrane or (b) that the movement of the empty transporter in response to potential steps is so fast that the pre-steady-state currents become indistinguishable from the capacitive currents. Our approach to decrease the turnover rate by lowering the temperature only reduced steady-state currents, but did not uncover a pre-steady-state-current component. Another possible reason for the lack of pre-steady-state currents could be that the turnover rate of PAT1 is much higher than that, for example, of PEPT1, and therefore a much smaller number of transporters generates the same rate of maximal currents as, for example, PEPT1. As a consequence of this, the charge movements induced by the reorientation of the transporters in response to potential steps would be too small to be detected – even at low temperature. That PAT1 could indeed have a very high turnover rate is supported by the following observations: (a) comparable inward currents after injection of equal amounts of cRNA of PAT1 and PEPT1 into oocytes can be obtained at least 1 day earlier in case of PAT1 and (b) capacitance measurements revealed a considerable increase of the membrane capacitance proportional to the transport current in oocytes expressing PEPT1, but a nearly unchanged membrane surface area in PAT1-expressing oocytes (results not shown). Taken together, our analysis does not, in its present state, permit a final conclusion to be drawn about the lack of detectable pre-steady-state currents in PAT1, but circumstantial evidence argues for an exceptionally high turnover rate.

PAT1 can transport in a reversed mode

The GPC and efflux experiments demonstrate, for the first time, that PAT1 is capable of transporting its substrates bidirectionally, with the direction of transport determined by the electrical and chemical proton gradient, as well as by the substrate gradient. Additionally, we observed a defined asymmetry in the conformation of the substrate-binding domain. Determinations of apparent K_m values revealed an identical substrate-binding pattern for the inward- and outward-faced transporters, but affinities for the PAT1-binding side when facing the cytosol are generally about 7-fold lower. This indicates a consistent conformational difference of the substrate-binding pocket in its inward- and outward-facing state that determines, for all substrates, an almost identical difference in affinity. In terms of the normal transport cycle, the lower affinity inside could promote the release of

the substrate into the cytosol. Whether PAT1-mediated outward transport of amino acid substrates plays a physiological role is currently not known. However, we show that outward transport can occur even at inside-negative membrane potentials, which resembles physiological conditions. The observed strong outward currents observed in the TEVC experiments after loading of oocytes with glycine is a consequence of the reversed driving forces, i.e. the pH and substrate gradients. PAT1-mediated amino acid transport has been shown to cause intracellular acidification of up to 1 pH unit [15] and therefore, after a longer substrate perfusion period, pH gradients could be outwardly directed. When the intracellular glycine concentration in oocytes perfused with 20 mM glycine was calculated on the basis of charge movement and using the Faraday constant (oocyte volume at 1.1 mm diameter: 700 nl with around 37 % aqueous phase) concentrations of 22–32 mM were determined, and it can be anticipated that these are even higher in the vicinity of the membrane. Under these conditions, PAT1 is capable of releasing substrates from the cells. Moreover, PAT1-mediated efflux of labelled L-proline from oocytes can be demonstrated, even in the absence of an outwardly directed pH gradient, and L-proline release was strongly stimulated by the presence of extracellular amino acid substrates with a half-maximal transactivation constant of around 1 mM. In man, typical extracellular concentrations of glycine, alanine and proline are in the range of 0.2–0.4 mM [29] and their concentrations, when added together, are therefore high enough to stimulate PAT1-mediated efflux of amino acids from cells. In addition, intracellular concentrations of PAT1 substrates such as glycine, but in particular of taurine or betaine, are fairly high, which would allow PAT1-mediated outward transport, for example, in the absence of a pH gradient or after membrane depolarization. Uptake and efflux of the osmolyte taurine via PAT1 could thereby contribute to the maintenance of a constant cell volume under hypo- or hyper-osmotic conditions. This proposed role of PAT1 may also be of relevance in non-epithelial cells with high intracellular concentrations of taurine and betaine, such as muscle, in which the PAT1 mRNA is expressed to a considerable extent [10]. Whether this is indeed a physiological function of PAT1 needs to be established.

In summary, PAT1 is an electrogenic H^+-coupled amino acid symporter with the capability for bidirectional amino acid transport. Proton and substrate binding affinities are strongly voltage-dependent, but the transport occurs most likely in an ordered fashion in which the proton binds before the amino acid does, followed by simultaneous substrate and proton translocation. Substrate interaction with the protein-binding sides in extracellular or intracellular orientation is determined by an asymmetry with a characteristic conformational difference and generally lower affinities in the outward-facing state. In contrast with many other co-transporters, the PAT1 transporter does not generate detectable pre-steady-state currents, either because of a symmetric charge distribution within the transporter protein or as a result of an exceptionally high turnover rate. Although the main function of PAT1 may be amino acid influx resulting in intracellular amino acid accumulation, under certain conditions PAT1 may even serve as an electrogenic proton/amino acid efflux transporter.

This work was supported by a grant (BO 1857/1) from the Deutsche Forschungsgemeinschaft (the German Research Council) to M.B. We thank Adelmar Stamfort very much for excellent technical assistance with the GPC technique.

REFERENCES

1 Saier, M. H. J. (2000) Families of transmembrane transporters selective for amino acids and their derivatives. Microbiology **146**, 1775–1795

2 Roigaard-Petersen, H., Jacobsen, C. and Iqbal, S. M. (1987) H^+–L-proline cotransport by vesicles from pars convoluta of rabbit proximal tubule. Am. J. Physiol. **253**, 15–20

3 Roigaard-Petersen, H., Jacobsen, C., Jessen, H., Mollerup, S. and Sheikh, M. I. (1989) Electrogenic uptake of D-imino acids by luminal membrane vesicles from rabbit kidney proximal tubule. Biochim. Biophys. Acta **984**, 231–237

4 Roigaard-Petersen, H., Jessen, H., Mollerup, S., Jorgensen, K. E., Jacobsen, C. and Sheikh, M. I. (1990) Proton gradient-dependent renal transport of glycine: evidence for vesicle studies. Am. J. Physiol. **258**, F388–F396

5 Thwaites, D. T., McEwan, G. T., Cook, M. J., Hirst, B. H. and Simmons, N. L. (1993) H^+-coupled Na^+-independent proline transport in human intestinal (Caco-2) epithelial cell monolayers. FEBS Lett. **333**, 78–82

6 Thwaites, D. T., McEwan, G. T., Brown, C. D., Hirst, B. H. and Simmons, N. L. (1993) Na^+-independent, H^+-coupled transepithelial β-alanine absorption by human intestinal Caco-2 cell monolayers. J. Biol. Chem. **268**, 18438–18441

7 Thwaites, D. T., Armstrong, G., Hirst, B. H. and Simmons, N. L. (1995) D-Cycloserine transport in human intestinal epithelial (Caco-2) cells: mediation by a H^+-coupled amino acid transporter. Br. J. Pharmacol. **115**, 761–766

8 Thwaites, D. T., McEwan, G. T. and Simmons, N. L. (1995) The role of the proton electrochemical gradient in the transepithelial absorption of amino acids by human intestinal Caco-2 cell monolayers. J. Membr. Biol. **145**, 245–256

9 Thwaites, D. T., Basterfield, L., McCleave, P. M., Carter, S. M. and Simmons, N. L. (2000) γ-Aminobutyric acid (GABA) transport across human intestinal epithelial (Caco-2) cell monolayers. Br. J. Pharmacol. **129**, 457–464

10 Boll, M., Foltz, M., Rubio-Aliaga, I. and Daniel, H. (2003) A cluster of proton/amino acid transporter genes in the human and mouse genomes. Genomics **82**, 47–56

11 Boll, M., Foltz, M., Rubio-Aliaga, I., Kottra, G. and Daniel, H. (2002) Functional characterization of two novel mammalian electrogenic proton-dependent amino acid cotransporters. J. Biol. Chem. **277**, 22966–22973

12 Chen, Z., Fei, Y. J., Anderson, C. M., Wake, K. A., Miyauchi, S., Huang, W., Thwaites, D. T. and Ganapathy, V. (2003) Structure, function and immunolocalization of a proton-coupled amino acid transporter (hPAT1) in the human intestinal cell line Caco-2. J. Physiol. (Cambridge) **546**, 349–361

13 Sagne, C., Agulhon, C., Ravassard, P., Darmon, M., Hamon, M., El Mestikawy, S., Gasnier, B. and Giros, B. (2001) Identification and characterization of a lysosomal transporter for small neutral amino acids. Proc. Natl. Acad. Sci. U.S.A. **98**, 7206–7211

14 Wreden, C. C., Johnson, J., Tran, C., Seal, R. P., Copenhagen, D. R., Reimer, R. J. and Edwards, R. H. (2003) The H^+-coupled electrogenic lysosomal amino acid transporter LYAAT1 localizes to the axon and plasma membrane of hippocampal neurons. J. Neurosci. **23**, 1265–1275

15 Boll, M., Foltz, M., Anderson, C. M., Oechsler, C., Kottra, G., Thwaites, D. T. and Daniel, H. (2003) Substrate recognition by the mammalian proton-dependent amino acid transporter PAT1. Mol. Membr. Biol. **20**, 261–269

16 Kottra, G. and Daniel, H. (2001) Bidirectional electrogenic transport of peptides by the proton-coupled carrier PEPT1 in *Xenopus laevis* oocytes: its asymmetry and symmetry. J. Physiol. (Cambridge) **536**, 495–503

17 Rubio-Aliaga, I., Boll, M., Foltz, D. M., Kottra, M. and Daniel, G. H. (2004) The proton/amino acid cotransporter PAT2 is expressed in neurons with a different subcellular localization than its paralog PAT1. J. Biol. Chem. **279**, 2754–2760

18 Daniel, H., Fett, C. and Kratz, A. (1989) Demonstration and modification of intervillous pH profiles in rat small intestine *in vitro*. Am. J. Physiol. **257**, G489–G495

19 Thwaites, D. T., Ford, D., Glanville, M. and Simmons, N. L. (1999) H^+/solute-induced intracellular acidification leads to selective activation of apical Na^+/H^+ exchange in human intestinal epithelial cells. J. Clin. Invest. **104**, 629–635

20 Golabek, A. A., Kida, E., Walus, M., Kaczmarski, W., Michalewski, M. and Wisniewski, K. E. (2000) CLN3 protein regulates lysosomal pH and alters intracellular processing of Alzheimer's amyloid-β protein precursor and cathepsin D in human cells. Mol. Genet. Metab. **70**, 203–213

21 Jauch, P. and Lauger, P. (1986) Electrogenic properties of the sodium–alanine cotransporter in pancreatic acinar cells: II. Comparison with transport models. J. Membr. Biol. **94**, 117–127

22 Mackenzie, B., Loo, D. D., Panayotova-Heiermann, M. and Wright, E. M. (1996) Biophysical characteristics of the pig kidney Na^+/glucose cotransporter SGLT2 reveal a common mechanism for SGLT1 and SGLT2. J. Biol. Chem. **271**, 32678–32683

23 Klamo, E. M., Drew, M. E., Landfear, S. M. and Kavanaugh, M. P. (1996) Kinetics and stoichiometry of a proton/myo-inositol cotransporter. J. Biol. Chem. **271**, 14937–14943

24 Stein, W. D. (1989) Kinetics of transport: analyzing, testing, and characterizing models using kinetic approaches. Methods Enzymol. **171**, 23–62

25 Eskandari, S., Loo, D. D., Dai, G., Levy, O., Wright, E. M. and Carrasco, N. (1997) Thyroid Na^+/I^- symporter. Mechanism, stoichiometry, and specificity. J. Biol. Chem. **272**, 27230–27238

26 Mackenzie, B., Loo, D. D., Fei, Y., Liu, W. J., Ganapathy, V., Leibach, F. H. and Wright, E. M. (1996) Mechanisms of the human intestinal H^+-coupled oligopeptide transporter hPEPT1. J. Biol. Chem. **271**, 5430–5437

27 Loo, D. D., Hirayama, B. A., Gallardo, E. M., Lam, J. T., Turk, E. and Wright, E. M. (1998) Conformational changes couple Na^+ and glucose transport. Proc. Natl. Acad. Sci. U.S.A. **95**, 7789–7794

28 Chaudhry, F. A., Schmitz, D., Reimer, R. J., Larsson, P., Gray, A. T., Nicoll, R., Kavanaugh, M. and Edwards, R. H. (2002) Glutamine uptake by neurons: interaction of protons with system A transporters. J. Neurosci. **22**, 62–72

29 Chih-Kuang, C., Shuan-Pei, L., Shyue-Jye, L. and Tuan-Jen, W. (2002) Plasma free amino acids in Taiwan Chinese: the effect of age. Clin. Chem. Lab. Med. **40**, 378–382

Received 6 September 2004/19 October 2004; accepted 26 October 2004
Published as BJ Immediate Publication 26 October 2004, DOI 10.1042/BJ20041519